Dendritic cells promote the spread of human T-cell leukemia virus type-1 via bidirectional interactions with CD4$^+$ T-cells

TakatoshiShimauchi[12] StephanCaucheteux[1] KatjaFinsterbusch[1#a] JocelynTurpin[3] FabienBlanchet[1#b] KristinLadell[1] KathyTriantafilou[1] MagdalenaCzubala[1] KazukiTatsuno[2] TammyEaster[1] ZahraAhmed[1] RebeccaBayliss[1] SvetlanaHakobyan[1] David A.Price[1] YoshikiTokura[2] VincentPiguet[145]

[1] Division of Infection and Immunity, Cardiff University School of Medicine, Cardiff, United Kingdom
[2] Department of Dermatology, Hamamatsu University School of Medicine, Hamamatsu, Japan
[3] Section of Virology, Department of Medicine, Imperial College London, London, United Kingdom
[4] Division of Dermatology, Women's College Hospital, Toronto, Canada
[5] Division of Dermatology, Department of Medicine, University of Toronto, Canada

ABSTRACT

Human T-cell leukemia virus type-1 (HTLV-1) propagates within and between individuals via cell-to-cell transmission, and primary infection typically occurs across juxtaposed mucosal surfaces during breastfeeding and sexual intercourse. It is therefore likely that dendritic cells (DCs) are among the first potential targets for HTLV-1. However, it remains unclear how DCs contribute to virus transmission and dissemination in the early stages of infection. We show that an HTLV-1-infected cell line (MT-2) and naturally-infected CD4$^+$ T-cells transfer p19$^+$viral particles to the surface of allogeneic DCs via cell-to-cell contacts. Similarly organized cell-to-cell contacts facilitate DC-mediated transfer of HTLV-1 to autologous CD4$^+$ T-cells. These findings shed light on the cellular structures involved in anterograde and retrograde transmission, and suggest a key role for DCs in the natural history and pathogenesis of HTLV-1 infection.

INTRODUCTION

Human T-cell leukemia virus type-1 (HTLV-1) causes adult T-cell leukemia/lymphoma (ATLL), HTLV-1-associated myelopathy/tropical spastic paraparesis (HAM/TSP), and HTLV-1-associated infective dermatitis (Fuzii et al., 2014; McGill et al., 2012; Uchiyama et al., 1977). The most severe clinical manifestation is ATLL, an aggressive and usually fatal lymphoproliferative disorder that develops in 1–5% of HTLV-1-infected individuals, typically after decades of apparent latency (Gessain and Cassar, 2012).

Primary infection occurs during intimate mucosal contact, suggesting a key role for dendritic cells (DCs) and/or Langerhans cells (LCs) in the transmission process (Shimauchi and Piguet, 2015). In line with this supposition, a number of studies have demonstrated that various DC subsets, including plasmacytoid DCs (pDCs), myeloid DCs (mDCs), and monocyte-

derived DCs (MDDCs), can be infected at low levels *in vitro* by both cell-free and cell-associated HTLV-1 (Alais et al. 2015; Ceccaldi et al., 2006; Jain et al., 2009; Jones et al., 2008; Lambert et al., 2009; Martin-Latil et al., 2012; Rizkallah et al., 2017; Valeri et al., 2010). It has also been shown that HTLV-1-infected DCs can transfer the virus to target CD4+ T-cells (Jain et al., 2009; Jones et al., 2008). These results are supported by *ex vivo* studies of DC subsets isolated from HTLV-1-infected individuals (Hishizawa et al., 2004; Macatonia et al., 1992; Makino et al., 1999). Thus, DCs are thought to play a key role in the early stages of infection, acting as a pivotal reservoir of transmissible virions that facilitates the dissemination of HTLV-1 via clonally expanded CD4+ T-cells.

Although DCs can be infected with HTLV-1 in a cell-free manner, efficient infection requires cell-to-cell contacts in the form of virological synapses (Igakura et al., 2003) and/or cellular conduits (Van Prooyen et al., 2010), potentially modulated by biofilm-like extracellular viral assemblies (Pais-Correia et al., 2010). HTLV-1-containing virological synapses are based on interactions between intercellular adhesion molecule-1 (ICAM-1) on the infected cell surface and leukocyte function-associated molecule-1 (LFA-1) on the target cell surface, which induce the accumulation of talin and polarization of the microtubule-organizing center (MTOC) towards the cell-to-cell contact zone (Igakura et al., 2003). Virological synapse formation can facilitate the transmission of HTLV-1 proteins and genomic RNAs to the target cell within two hours (Igakura et al., 2003). Viral particles also congregate transiently in carbohydrate-rich extracellular assemblies (Pais-Correia et al., 2010). These unique biofilm-like structures can be transferred rapidly between infected and target CD4+ T-cells (Pais-Correia et al., 2010). However, it is remains unclear whether virological synapses or biofilm-like extracellular viral assemblies are involved in DC-mediated transmission of HTLV-1.

In this study, we used confocal and electron microscopy to show that cell-to-cell contacts mediate virus transfer between HTLV-1-infected CD4+ T-cells and the surface membrane of DCs. Moreover, Alu-PCR and high-throughput integration site analysis revealed little evidence for proviral integration in DCs. In addition, we show that DCs can transfer HTLV-1 to autologous CD4+ T-cells *in trans*. Collectively, these findings demonstrate that cell-to-cell contacts play a key role in DC-mediated transmission of HTLV-1.

RESULTS

HTLV-1-infected cells transfer viruses to immature DCs via cell-to-cell contacts

Virological synapses facilitate the transmission of HTLV-1 from infected to uninfected CD4+T-cells (Igakura et al., 2003). However, little is known about the cell-to-cell contact structures that mediate viral transfer between HTLV-1-infected CD4+ T-cells and DCs. To address this issue, we first cultured primary human immature monocyte-derived DCs (iDCs) for 96 hr in the presence or absence of HTLV-1-producing T-cell line MT-2. Transmission electron microscopy (TEM) showed that iDCs formed virological synapse-like contacts with MT-2 cells (Figure 1a). Moreover, scanning electron microscopy (SEM) demonstrated that iDCs adjacent to MT-2 cells formed reduced numbers of filopodia, some of which extended in prolonged tubes resembling filopodial bridges to contact the MT-2 cells (Figure 1b). In contrast, iDCs cultured in the absence of MT-2 cells extended their filopodia to the periphery (Figure 1a and b).

Next, we co-cultured iDCs with MT-2 cells for 48 hr and performed confocal immunofluorescence analysis. The images demonstrated that MT-2 cells expressed high surface levels of HTLV-1 p19 Gag within a carbohydrate-rich matrix identified using the Concanavalin A viruses were polarized toward the contact zones, indicating virological synapse formation (Figure 1d). Other images further showed that the transferred viruses remained close to the surface of iDCs (Figure 1e).

Cell-to-cell contact is required for virus transmission between HTLV-1-infected cells and DCs

To quantify HTLV-1 transmission from MT-2 cells to iDCs and lipopolysaccharide (LPS)-matured DCs (mDCs), we co-cultured iDCs with or without MT-2 cells in the presence or absence of LPS. After 48 hr, we analyzed intracellular expression levels of p19 Gag in neuropilin-1 (NRP-1)+ CD25– Live/Dead– CD1a+ iDCs/mDCs by flow cytometry (Figure 2a). Cell viability was comparable between the two conditions (Figure 2b). The frequencies of p19+ CD1a+ iDCs were comparable across time points in the presence of MT-2 cells, whereas iDCs cultured in the absence of MT-2 cells were negative for p19 Gag (Figure 2c). In contrast, virus transmission to mDCs was significantly enhanced after 48 hr in the presence of LPS (Figure. 2d). Parallel assays conducted across transwell membranes demonstrated that cell-to-cell contacts were required to mediate efficient virus transmission (Figure. 2e).

Naturally HTLV-1-infected CD4+ T-cells transfer viruses to DCs via cell-to-cell contacts

MT-2 cells have a high proviral load (PVL) and do not necessarily recapitulate the physiological characteristics of CD4+ T-cells *in vivo*. To address this potential caveat, we prepared HTLV-1-infected CD4+ T-cells from five patients with ATLL, two patients with HAM/TSP, and two asymptomatic carriers of HTLV-1. Allogeneic CD4+ T-cells from healthy volunteers were used as negative controls. Intracellular p19 Gag was expressed at high levels in CD4+ T-cells isolated from some ATLL patients (case 1 and case 3) relative to CD4+ T-cells from other HTLV-1+ groups or healthy controls (Figure 3a, and b). In co-culture experiments performed over 48 hr in the presence of LPS, p19 Gag was detected in mDCs incubated with highly infected CD4+ T-cells from an ATLL patient (case 1) (Figure 3c and d). In contrast, no virus transmission was detected in the presence of CD4+ T-cells with low levels of intracellular p19 Gag (Figure 3d). Thus, ATLL tumor cells producing high levels of HTLV-1 can transfer virions to allogeneic DCs.

To determine if HTLV-1-infected CD4+ T-cells with low levels of intracellular p19 Gag can transfer viruses to DCs, we performed similar experiments using confocal microscopy instead of flow cytometry. As expected, low virus producing CD4+ T-cells from ATLL (case 2) and HAM/TSP (case 2) patients expressed p19+ viral particles and transferred them to thesurface of iDCs at the contact zone (Figure 3e, 3f). While, no p19+ viral particles were detected in healthy allogeneic CD4+ T-cells (Figure 3g). Thus, naturally infected CD4+ T-cells expressing low levels of intracellular p19 Gag can transfer HTLV-1 to DCs.

Cell-to-cell contacts with HTLV-1-infected T-cells lead to *trans* infection of DCs

Next, we examined the possibility that p19+ viruses detected on the surface of DCs were produced *de novo* after transfer from MT-2 cells. The HTLV-1 transactivator protein Tax is not transferred from infected to target cells, but it is expressed in target cells after viral integration (Jones et al., 2008). We therefore analyzed intracellular expression levels of p19 Gag and Tax in NRP-1+ CD1a+ mDCs by flow cytometry. Our results showed that LPS-induced mDCs did not express intracellular Tax (Figure 4a and b).

To confirm this finding, which suggests viral capture rather than productive infection, we used Alu-PCR to analyze the integration of HTLV-1 proviral DNA. After overnight co-culture, iDCs were separated from MT-2 cells using CD25 MicroBeads (Figure 4c). No *gag*

amplification signals were detected in genomic DNA from HTLV-1+ and control iDCs (Figure 4d, lanes 2, 3, 5, and 6). In contrast, genomic DNA extracted from MT-2 cells as a positive control yielded clear *gag* amplification signals (Figure 4d, lane 1). Similar results were obtained with samples from five different donors. Nonetheless, HTLV-1+ iDCs from donor 1 and donor 2 exhibited PVLs of 0.79 % and 4.16 %, respectively (Figure 4d). We therefore performed unique integration site (UIS) mapping by high throughput sequencing (HTS) (Meekings et al., 2008). We detected 33 (donor 1) and 36 (donor 2) UISs in total, more than half of which corresponded with known UISs in MT-2 cells. Moreover, the nine most abundant UISs corresponded with known UISs in MT-2 cells (Figure 4e). Accordingly, 16 UISs in donor 1 and 17 UISs in donor 2, all of which were singletons, did not match known UISs in MT-2 cells. The proportion of singletons was higher in iDCs compared with MT-2 cells, and the corresponding oligoclonality index was lower (Figure 4e). In addition to previously known UISs in MT-2 cells, donor 1 and 2 shared two other common UISs (chromosome 2 at position 60971860 and chromosome 6 at position 138426919). Our HTS analysis therefore suggests that much of the measured PVL in iDCs corresponded with low numbers of passenger MT-2 integrants. Collectively, these data indicate that DCs capture HTLV-1, but are not productively infected with HTLV-1.

DC-mediated HTLV-1 transfer to autologous CD4+ T-cells *in trans*

To test the idea that, DCs can re-transfer viruses to CD4+ T-cells *in trans*, we co-cultured HTLV-1+ iDCs/mDCs with uninfected autologous CD4+ T cells for 3 hr or 48 hr and measured the frequencies of p19+ CD4+ T-cells in the CD3+ CD4+ and DC-SIGN– CD25– populations (Figure 5a). No p19+ CD4+ T-cells were detected after co-culture with uninfected DCs (Figure 5a). In contrast, HTLV-1+ iDCs and HTLV-1+ mDCs both transferred virus to uninfected autologous CD4+ T-cells within 3 hr (Figure 5a). Thus, cell-to-cell contacts contribute to DC-mediated HTLV-1 transfer to CD4+ T-cells.

To confirm these findings, we used confocal and electron microscopy to visualize DC-mediated transfer of HTLV-1 to CD4+ T-cells. TEM showed that HTLV-1+ iDCs formed reduced numbers of filopodia in the presence of HTLV-1+ MT-2 cells, but were capable of making intimate contacts with CD4+ T-cells (Figure 5b left panel). SEM also demonstrated that CD4+ T-cells contacted the surface membranes of HTLV-1+ iDCs (Figure 5b right

upper and lower panel). After 48 hr, HTLV-1+ iDCs formed cell-to-cell contacts with autologous CD4+ T-cells via filopodial extensions (Figure 5c). In agreement with our flow cytometric analysis, the confocal images further revealed that p19+ viral particles were transferred from DCs to CD4+ T-cells within 3 hr (Figure 5d, 5f). Moreover, p19+ viral particles were no longer detectable in the DC-T-cell contact zone after 48 hr, instead localizing to the T-cell side of the contact zone or the T-cell surface (Figure 5e, 5g). In contrast to HTLV-1+ iDCs, control iDCs formed numerous filopodia and also formed contacts with CD4+ T-cells. No p19+ viral particles were detected in control mDCs. Collectively, these data show that cell-to-cell contacts contribute to DC-mediated HTLV-1 transfer to CD4+ T-cells.

DISCUSSION

In this study, we show that cell-to-cell contacts facilitate the bidirectional transfer of HTLV-1 between CD4+ T-cells and DCs. This process is far more efficient than cell-free transmission, and does not require productive infection of DCs. These findings suggest a key role for DCs in the acquisition and dissemination of HTLV-1.

Previous studies have shown that HTLV-1 binds first to heparan sulfate proteoglycans and NRP-1, and then to glucose transporter type 1 (Glut-1), on target CD4+ T-cells (Ghez et al., 2006; Jones et al. 2005; Lambert et al., 2009; Manel et al., 2003). In the case of DCs, HTLV-1 can bind also to DC-SIGN (Jain et al., 2009). We confirmed that both NRP-1 and DC-SIGN were highly expressed on DCs, but found that Glut-1 expression was lower compared with Jurkat cells or activated CD4+ T-cells. In addition, ICAM-1 was highly expressed on MT-2 cells and DCs, whereas LFA-1 was weakly expressed on MT-2 cells and DCs compared with activated CD4+ T-cells. Virological synapses between HTLV-1-infected CD4+ T-cells and DCs may therefore be structurally incomplete, which could explain the low efficiency of productive viral infection in target DCs.

It has been reported previously that HTLV-1 virions are transferred at virological synapses via biofilm-like extracellular viral assemblies (Pais-Correia et al., 2010). Our findings provide support for this notion in terms of a synergistic interaction, but also suggest a degree of separability between these modes of transmission. The transfer of viral particles is not a specific property of DCs. To evaluate the efficiency of viral transfer by important cell types

involved in HTLV-1 infection, we also performed HTLV-1 transfer assays by using both iDCs/mDCs and CD4+ T-cells to target autologous CD8+ T-cells. However, there was no significant difference between DCs-mediated and CD4+ T-cell-mediated virus transmission to autologous CD8+ T-cells. Thus, the transfer of HTLV-1 viral particles is not a specific property of dendritic cells. However, the data strongly suggests that DCs can transfer the virus with the same efficiency as CD4+ T-cells, which is thought to be a major virus transmitter.

In contrast to our results, a recent using a different experimental model demonstrated that DCs can be infected by to HTLV-1 infected lines and that purified cell-free HTLV-1 in association with biofilms is more infectious than cell-free HTLV-1 in isolation (Alais et al., 2015). They also demonstrated that MDDCs were more susceptible to HTLV-1 infection than their autologous lymphocytes after contact with HTLV-1 infected and producing cell line, C91PL (Alais et al., 2015). Furthermore, the authors reported that HTLV-1 viral transmission from DCs to T-cells could result from transmission of newly synthesized virus from productively infected iDCs and mDCs (Rizkallah et al., 2017). For HTLV-1 infection and transmission model, the pretreatment of virus producing cell lines, MT-2 or C91PL cells with g irradiation or mitomycin C increases their efficiency to infect the target cells *in vitro*. However, these sublethal conditions may also reshape the structure of extracellular viral assemblies (Pais-Correia et al, 2010). In order to evaluate the nature of DC-T cells contacts, we used live MT-2 cells, as commonly used cell line, as well as live naturally infected CD4+T-cells without any pretreatment in our study. However, it remains unclear whether or not bioflim-like extracellular viral assemblies exist *in vivo*, and further studies are therefore warranted to understand the role of these structures in the natural history of HTLV-1 infection.

As in the case of HIV-1 (Geijtenbeek et al., 2000; McDonald et al., 2003; Turville et al., 2004), we found that LPS-induced mDCs captured and transferred HTLV-1 to CD4+ T-cells *in trans* more efficiently than iDCs. The results were also consistent with the data from a recent paper demonstrating that LPS-induced mDCs increases HTLV-1 uptake (Rizkallah et al., 2017). HIV-1 particles bind randomly to plasma membranes and eventually become concentrated into distinct, invaginated pockets on the surface of mDCs (Izquierdo-Useros et al., 2011). Sialic acid-binding Ig-like lectin 1 (Siglec-1, CD169) is also highly expressed on mDCs and can bind HIV-1, facilitating viral spread to target CD4+ T-cells (Sewald et al., 2015). It is therefore possible

that membrane trafficking effects and/or other surface receptors could play an important role in DC-mediated HTLV-1 transmission via biofilm-like extracellular viral assemblies.

In addition to viral entry constraints, DCs are known to possess cell-specific restriction factors, which may further limit proviral integration. These include tripartite motif-5 alpha (TRIM-5 alpha), apolipoprotein B mRNA-editing enzyme-catalytic polypeptide-like 3G or 3F (APOBEC3G/3F), bone marrow stromal cell antigen-2 (BST-2, also known as tetherin, CD317, or HM1.24), and sterile alpha motif and hemidesmosome domain-containing protein 1 (SAMHD1) (Ahmed et al., 2013). SAMHD1 was identified as a critical post-entry restriction factor that limits HIV-1 infection in myeloid DCs, but not in LCs, via depletion of the cellular deoxynucleoside triphosphate pool, which inhibits reverse transcription of viral RNA (Czubala et al., 2016; Goldstone et al., 2011; Lahouassa et al., 2012). It has also been reported that SAMHD1 can limit HTLV-1 infection in monocytes (Sze et al. 2013), but this remains controversial (Gramberg et al., 2013). We also investigated whether down-regulation of SAMHD1 can enhance HTLV-1 infection in DCs. However, we found equivalent frequencies of p19+ or Tax+ DCs and equivalent levels of phosphorylated interferon regulatory factor 3 (IRF3) in the presence or absence of SAMHD1. Although we cannot exclude the possibility of other viral restriction mechanisms, we suggest that HTLV-1 *trans*-infection of DCs plays a key role in the early stages of virus transmission.

In conclusion, we show here that cell-to-cell contacts possibly involving biofilm-like extracellular viral assemblies mediate the bidirectional transfer of HTLV-1 between CD4+T-cells and the surface membrane of DCs. These findings suggest a key role for DCs in the early propagation of HTLV-1, akin to that described for HIV-1 (Piguet and Steinman, 2007; Piguet et al., 2014).

MATERIALS AND METHODS

Cells and cell culture

Buffy coats were obtained from healthy donors via the Welsh Blood Bank. CD14+ monocytes were isolated and differentiated to iDCs as described previously (Blanchet et al., 2013). For use as autologous targets, CD4+ T-cells or CD8+ T-cells were purified using a CD4+ T-cell and CD8+ T-cell Isolation Kit II (Mitenyi Biotec), stimulated with 1 microg/ml

phytohemagglutinin (PHA), and maintained in RPMI 1640 (Gibco) supplemented with 100 U/mL recombinant human IL-2 (rhIL-2, Mitenyi Biotec). For use in *ex vivo* studies, uninfected and HTLV-1-infected CD4+ T-cells were purified as above and cultured overnight in supplemented RPMI 1640. The human T-cell acute lymphoblastic leukemia (T-ALL), Jurkat (E6.1), and MT-2 cell lines were maintained in supplemented RPMI 1640. HEK293T cells were cultured in DMEM (Gibco) supplemented with 10% fetal calf serum, 100 IU/mL penicillin, and 100 ug/mL streptomycin. All cell lines used in this study tested negative for *Mycoplasma*. The MT-2 cell line was kindly provided by Prof. Toshiki Watanabe (University of Tokyo) and Prof. Charles Bangham (Imperial College London).

HTLV-1 transfer from CD4+ T-cells to DCs

On day 5 or 6 post-differentiation, 1 x 105 iDCs were cultured in round-bottom 96-well plates with 1 x 105 MT-2, Jurkat, or allogeneic CD4+ T-cells in 100 uL of IMDM with GlutMax (Gibco). mDCs were generated via the addition of LPS (1 mg/mL, InvivoGen). After 48 hr, cells were processed for flow cytometric analyses or confocal microscopy studies. In some experiments, cell populations were separated across transwell chambers in 24-well culture plates (6.5 mm Transwell with 0.4 um Pore Polyester Membrane Insert, Corning).

Ethics statement

Experimental protocols were approved by Cardiff University Research Ethics Committee. Sample collection was approved by the Ethics Committee of Hamamatsu University School of Medicine (E23-173). Written informed consent was obtained from all patients, and the study was conducted in accordance with the principles of the Declaration of Helsinki

Abbreviations:

HTLV-1, Human T-cell leukemia virus type-1; DCs, dendritic cells; ATLL, adult T-cell leukemia/lymphoma; HAM/TSP, HTLV-1-associated myelopathy/tropical spastic paraparesis; iDCs, immature dendritic cells; mDCs, mature dendritic cells; LPS, lipopolysaccharide; PVL, proviral load; NRP-1, neuropilin-1; UIS, unique integration site; HTS, high throughput sequencing; Glut-1, glucose transporter type 1; SAMHD1, sterile alpha motif and hemidesmosome domain-containing protein 1; TEM, transmission electron microscopy; SEM, scanning electron microscopy; ConA, Concanavalin A;

REFERENCES

1. Ahmed Z, Czubala M, Blanchet F, Piguet, V. HIV impairment of immune responses in dendritic cells. Adv Exp Med Biol 2013;762:201-38.

2. Alais S, Mahieux R, Dutartre H. Viral source-independent high susceptibility of dendritic cells to human T-cell leukemia virus type 1 infection compared to that of T lymphocytes. J Virol 2015;89:10580-90.

3. Blanchet FP, Stalder R, Czubala M, Lehmann M, Rio L, Mangeat B, et al. TLR-4 engagement of dendritic cells confers a BST-2/tetherin-mediated restriction of HIV-1 infection to CD4+ T cells across the virological synapse. Retrovirology 2013;10:6.

4. Ceccaldi PE, Delebecque F, Prevost MC, Moris A, Abastado JP, Gessain A, et al. DC-SIGN facilitates fusion of dendritic cells with human T-cell leukemia virus type 1-infected cells. J Virol 2006;80:4771-80.

5. Czubala MA, Finsterbusch K, Ivory MO, Mitchell JP, Ahmed Z, Shimauchi T, et al. TGFb induces a SAMHD1-Independent Post-Entry Restriction to HIV-1 Infection of Human Epithelial Langerhans Cells. J Invest Dermatol 2016;136: 1981-9.

6. Fuzii HT, daSilva Dias GA, de Barros RJ, Falcão LF, Quaresma JA. Immunopathogenesis of HTLV-1-associated myelopathy/tropical spastic paraparesis (HAM/TSP). Life Sci 2014;104:9-14.

7. Geijtenbeek TB, Kwon DS, Torensma R, van Villet SJ, van Duijnhoven GC, Middel J, et al. DC-SIGN, a dendritic cell-specific HIV-1-binding protein that enhances trans-infection of T cells. Cell 2000;100:587-97.

8. Ghez D, Lepelletier Y, Lambert S, Fourneau JM, Blot V, Janvier S, et al. Neuropilin-1 is involved in human T-cell lymphotropic virus type 1 entry. J Virol 2006;80:6844-54.

9. Goldstone DC, Ennis-Adeniran V, Hedden JJ, Groom HC, Rice GI, Christodoulou E, et al. HIV-1 restriction factor SAMHD1 is a deoxynucleoside triphosphate triphosphohydrolase. Nature 2011;480:379-82.

10. Gramberg T, Kahle T, Bloch N, Wittmann S, Mullers E, Daddacha W, et al. Restriction of diverse retroviruses by SAMHD1. Retrovirology 2013;**10**:26.

11. Gessain A, Cassar O. Epidemiological aspects and world distribution of HTLV-1 infection. Front Microbiol 2012;15:388.

12. Hishizawa M, Imada K, Kitawaki T, Ueda M, Kadowaki N, Uchiyama T. Depletion and impaired interferon-alpha-producing capacity of blood plasmacytoid dendritic cells in human T-cell leukaemia virus type I-infected individuals. Br J Haematol 2004;125:568-75.

13. Igakura T, Stinchcombe JC, Goon PK, Taylor GP, Weber JN, Griffiths GM, et al. Spread of HTLV-I between lymphocytes by virus-induced polarization of the cytoskeleton. Science 2003;299:1713-16.

14. Izquierdo-Useros N, Esteban O, Rodriguez-Plata MT, Erkizia I, Prado JG, Blanco J, et al. Dynamic imaging of cell-free and cell-associated viral capture in mature dendritic cells Traffic 2011;12:1702-13.

15. Jain P, Manuel SL, Khan ZK, Ahuja J, Quann K, Wigdahl B. DC-SIGN mediates cell-free infection and transmission of human T-cell lymphotropic virus type 1 by dendritic cells. J Virol 2009;83:10908-21.

16. Jones KS, Petrow-Sadowski C, Bertolette DC, Huang Y, Ruscetti FW. Heparan sulfate proteoglycans mediate attachment and entry of human T-cell leukemia virus type 1 virions into CD4+ T cells. J Virol 2005;79:12692-702.

17. Jones KS, Petrow-Sadowski C, Huang YK, Bertolette DC, Ruscetti FW. Cell-free HTLV-1 infects dendritic cells leading to transmission and transformation of CD4(+) T cells. Nat Med 2008;14:429-36.

18. Lahouassa H, Daddacha W, Hofmann H, Ayinde D, Logue EC, Dragin L, et al. SAMHD1 restricts the replication of human immunodeficiency virus type 1 by depleting the intracellular pool of deoxynucleoside triphosphates. Nat Immunol 2012;13:223-8.

19. Lambert S, Bouttier M, Vassy R, Seigneuret M, Petrow-Sadowski C, Janvier S, et al. HTLV-1 uses HSPG and neuropilin-1 for entry by molecular mimicry of VEGF165. Blood 2009;113:5176-85.

20. Macatonia SE, Cruickshank JK, Rudge P, Knight SC. Dendritic cells from patients with tropical spastic paraparesis are infected with HTLV-1 and stimulate autologous lymphocyte proliferation. AIDS Res Hum Retroviruses 1992;8:1699-706.

21. Makino M, Shimokubo S, Wakamatsu SI, Izumo S, Baba M. The role of human T-lymphotropic virus type 1 (HTLV-1)-infected dendritic cells in the development of HTLV-1-associated myelopathy/tropical spastic paraparesis. J Virol 1999;73:4575-81.

22. Manel N, Kim FJ, Kinet S, Taylor N, Sibbon M, Battini JL. The ubiquitous glucose transporter GLUT-1 is a receptor for HTLV. Cell 2003;115:449-59.

23. Martin-Latil S, Gnädig NF, Mallet A, Desdouits M, Guivel-Behhassine F, Jeannin P, et al. Transcytosis of HTLV-1 across a tight human epithelial barrier and infection of subepithelial dendritic cells. Blood 2012;120:572-80.

24. McDonald D, Wu L, Bohks SM, KewalRamani VN, Unutmaz D, Hope TJ. Recruitment of HIV and its receptors to dendritic cell-T cell junctions. Science 2003;300:1295-7.

25. McGill NK, Vyas J, Shimauchi T, Tokura Y, Piguet V. HTLV-1-associated infective dermatitis: updates on the pathogenesis. Exp Dermatol 2012;21:815-21.

26. Meekings KN, Leipzig J, Bushman FD, Taylor GP, Bangham CR. HTLV-1 integration into transcriptionally active genomic regions is associated with proviral expression and with HAM/TSP. PLoS Pathog 2008;4:e1000027.

27. Pais-Correia AM, Sachse M, Guadagnini S, Robbiati V, Lasserre R, Gessain A, et al. Biofilm-like extracellular viral assemblies mediate HTLV-1 cell-to-cell transmission at virological synapses. Nat Med 2010;16:83-9. Piguet V, Steinman RM. The interaction of HIV with dendritic cells: outcomes and pathways. Trends Immunol 2007;28:503-10.

28. Piguet V, Caucheteux SM, Iannetta M, Hosmalin A. Altered antigen-presenting cells during HIV-1 infection. Curr Opin HIV AIDS 2014;9:478-84.

29. Rizkallah G, Alais S, Futsch N, Tanaka Y, Journo C, Mahieux R, et al. Dendritic cell maturation, but not type I interferon exposure, restricts infection by HTLV-1, and viral transmission to T-cells. PLoS Pathog 2017;13:e1006353.

30. Sewald X, Ladinsky MS, Uchil PD, Beloor J, Pi R, Hermann C, et al. Retroviruses use CD169-mediated trans-infection of permissive lymphocytes to establish infection. Science 2015;350:563-7.

31. Shimauchi T, Piguet V. DC-T cell virological synapses and the skin: novel perspectives in dermatology. Exp Dermatol 2015;24:1-4.

32. S ze A, Belgnaoui SM, Olagnier D, Lin R, Hiscott J, van Grevenynghe J. Host restriction factor SAMHD1 limits human T cell leukemia virus type 1 infection of monocytes via STING-mediated apoptosis. Cell Host Microbe 2013;14:422-34.

33. Turville SG, Santos JJ, Frank I, Cameron PU, Willkinson J, Miranda-Saksena M, et al. Immunodeficiency virus uptake, turnover, and 2-phase transfer in human dendritic cells. Blood 2004;103:2170-9.

34. Uchiyama T, Yodoi J, Sagawa K, Takatsuki K, Uchino H. Adult T-cell leukemia: clinical and hematologic features of 16 cases. Blood 1977;50:481-92.

35. Valeri VW, Hryniewicz A, Andresen V, Jones K, Fenizia C, Bialuk I, et al. Requirement of the human T-cell leukemia virus p12 and p30 products for infectivity of human dendritic cells and macaques but not rabbits. Blood 2010;116: 3809-17.

36. Van Prooyen N, Gold H, Andresen V, Schwartz O, Jones K, Ruscetti F, et al. Human T-cell leukemia virus type 1 p8 protein increases cellular conduits and virus transmission. Proc Natl Acad Sci U S A 2010;107:20738-43.

Figure 1. Virus transmission from HTLV-1-producing MT-2 cells to iDCs via cell-to-cell contacts.

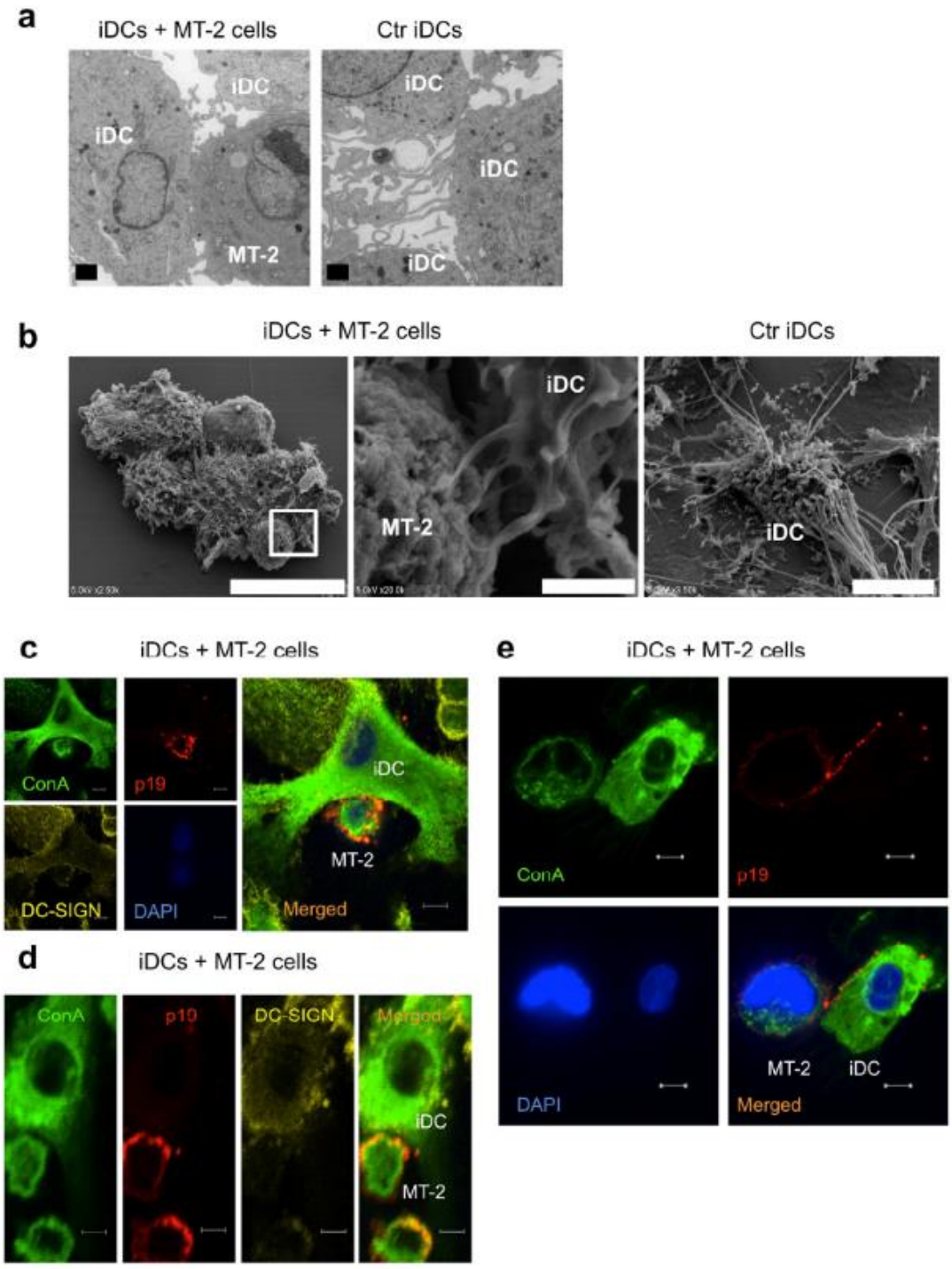

(**a**) TEM images of cell-to-cell contacts between iDCs and MT-2 cells, and control iDCs cultured in the absence of MT-2 cells. Scale bars = 1 mm. (**b**) SEM images of cell-to-cell contacts between iDCs and MT-2 cells, and control iDCs cultured in the absence of MT-2 cells. The highlighted area in left panel is enlarged in middle panel. Scale bars = 20 mm (left), 2 mm (middle**)**, 10 mm (right). (**c**–**e**) Confocal immunofluorescence images of cell-to-cell contacts between iDCs and MT-2 cells. Lectin-ConA (green), p19 Gag (red), CD3 (yellow), DAPI (nucleus, blue). Scale bars = 5 mm. TEM, transmission electron microscopy; SEM, scanning electron microscopy; iDCs, immature dendritic cells; ConA, Concanavalin A.

Figure 2. Quantification of HTLV-1 transmission from MT-2 cells to iDCs/mDCs via cell-to-cell contacts.

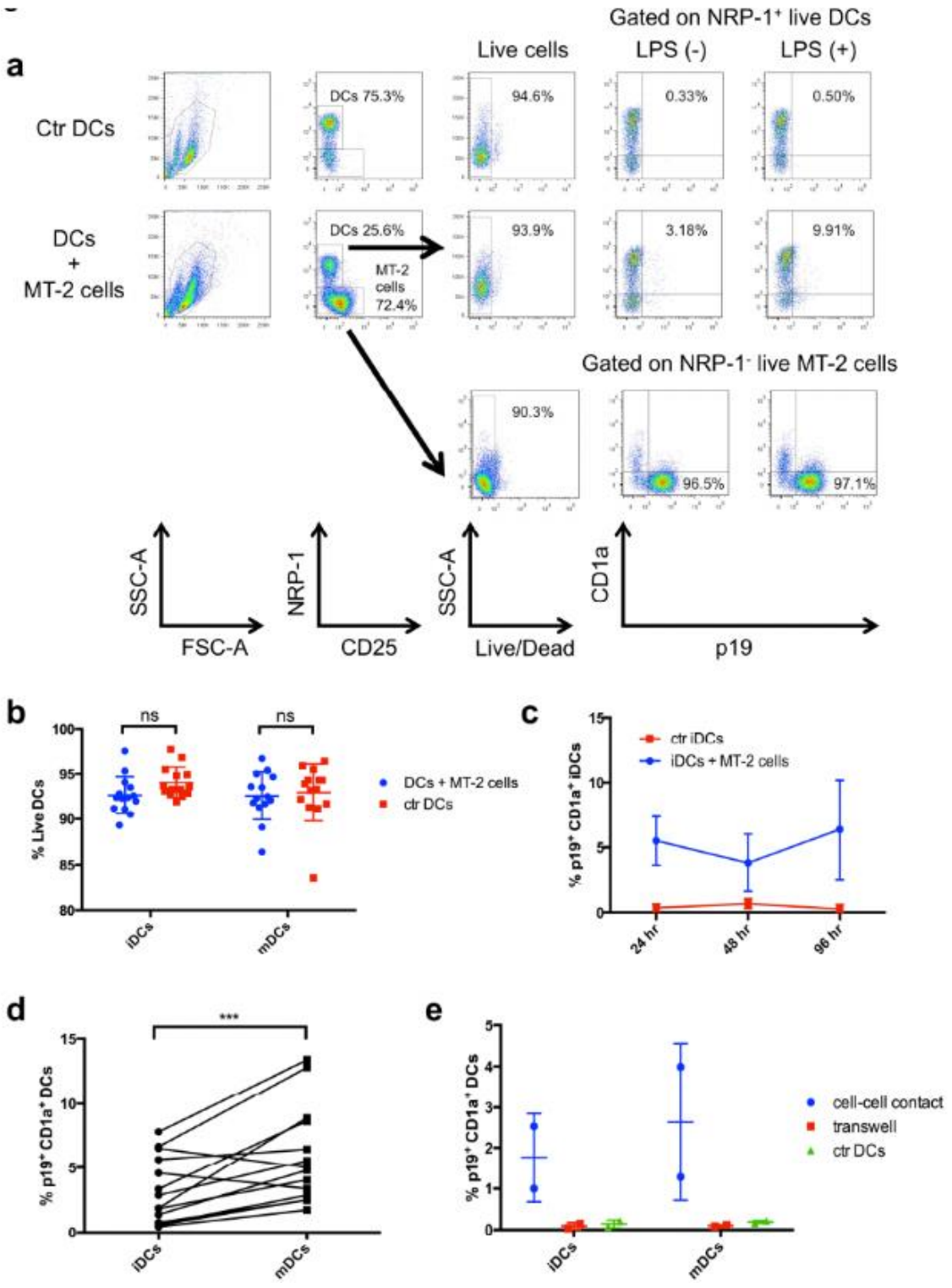

(**a**) iDCs were co-cultured for 48 hr with or without MT-2 cells in the presence or absence of LPS, and intracellular expression of p19 Gag in NRP-1+ CD25–Live/Dead– iDCs/mDCs was quantified by flow cytometry. (**b**) Comparison of cell viability across experimental conditions (n = 14). (**c**) Percentages of p19+ CD1a+ iDCs co-cultured for 24, 48, or 72 hr with or without MT-2 cells (n = 3). (**d, e**) Percentages of p19+ CD1a+iDCs/ mDCs co-cultured for 48 hr with MT-2 cells in the presence or absence of LPS (n = 14) or in the presence or absence of a transwell membrane (n = 2). Error bars indicate mean ± standard deviation. ****p* < 0.005; ns, not significant. iDCs, immature dendritic cells; mDCs, mature dendritic cells; NRP-1, neuropilin-1; LPS, lipopolysaccharide

Figure 3. Quantification of HTLV-1 transmission fromnaturally infected CD4+ T-cells to allogeneic DCs via cell-to-cell contacts.

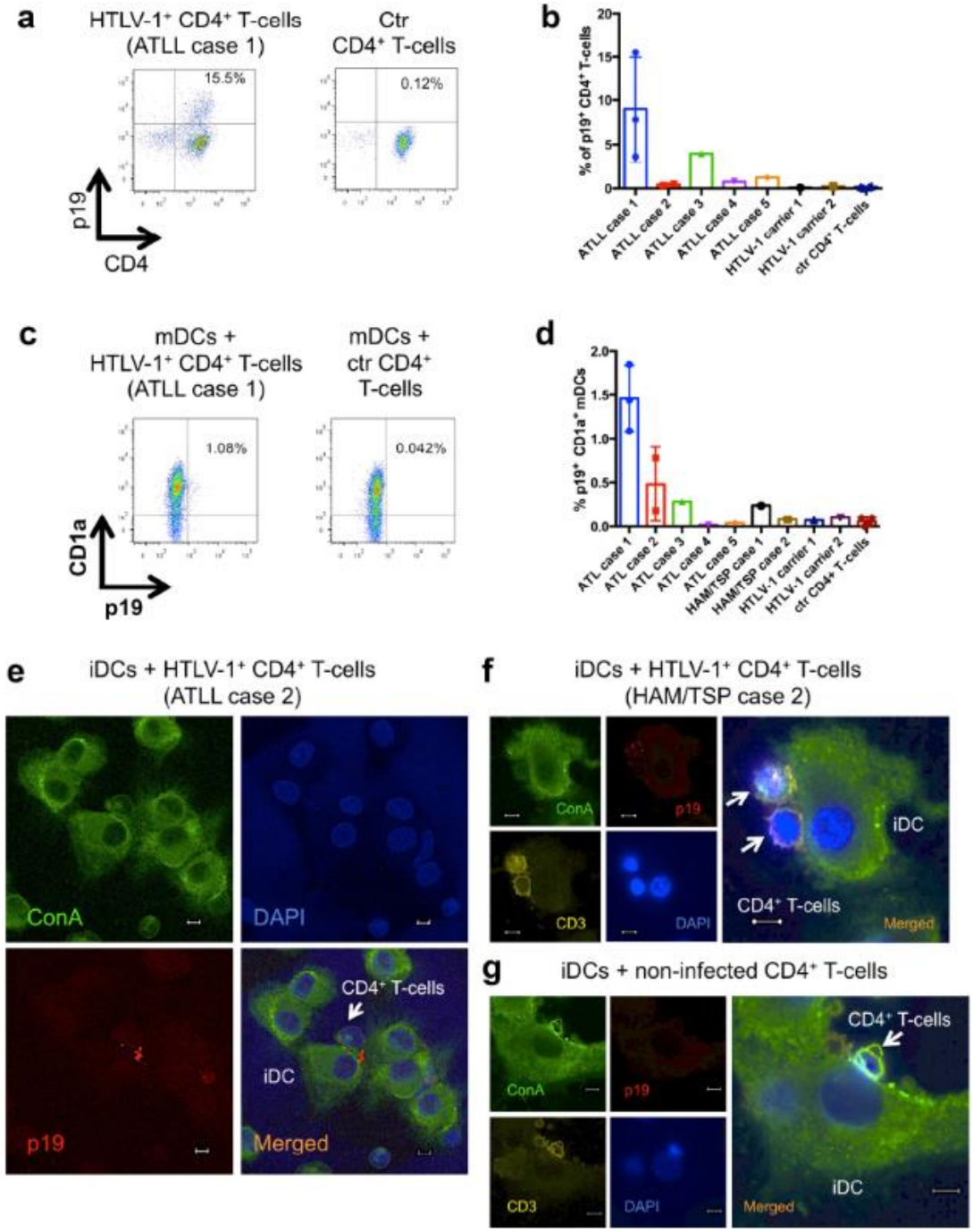

(**a, b**) Representative flow cytometry plots and composite data showing intracellular p19 Gag expression in CD4+ T-cells purified from HTLV-1-infected individuals (n = 7) and healthy donors (n = 4). (**c, d**) Representative flow cytometry plots and composite data showing intracellular p19 Gag expression in LPS-induced mDCs co-cultured for 48 hr with CD4+ T-cells purified from patients with ATLL (n = 5), HAM/TSP (n = 2), asymptomatic carriers of HTLV-1 (n = 2), and healthy donors (n = 4). Error bars indicate mean ± standard deviation. (**e**-**g**) Confocal immunofluorescence images of cell-to-cell contacts between iDCs and CD4+ T-cells purified from a patient with ATLL, HAM/TSP, and healthy donor. Lectin-ConA (green), p19 Gag (red), CD3 (yellow), DAPI (nucleus, blue). Scale bars = 5 mm. DCs, dendritic cells; LPS, lipopolysaccharide; mDCs, mature dendritic cells; NRP-1, neuropilin-1; ConA, Concanavalin A

Figure 4. *Trans*-infection of DCs via cell-to-cell contacts with HTLV-1-infected T-cells.

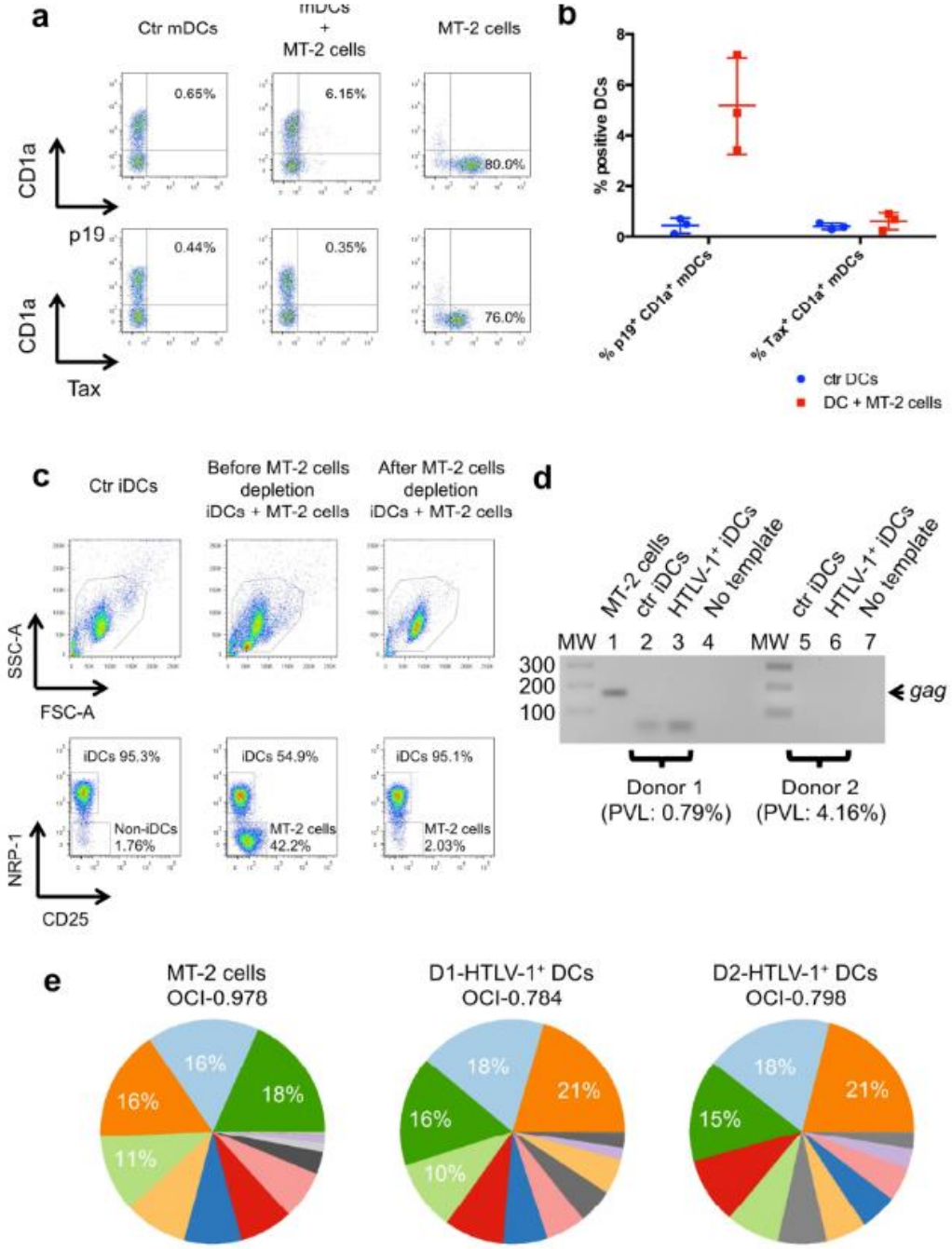

(**a, b**) Representative flow cytometry plots and composite data showing percentages of p19+ or Tax+ mDCs co-cultured with or without MT-2 cells (n = 3). Error bars indicate mean ± standard deviation. (**c**) Representative flow cytometry plots showing purification of HTLV-1+ iDCs from MT-2 cells using CD25 MicroBeads. (**d**) Representative Alu-PCR analysis of HTLV-1 proviral integration in genomic DNA extracted from HTLV-1+ iDCs (lanes 3 and 6), control iDCs (lanes 2 and 5), and MT-2 cells (lane 1). No template controls are shown in lanes 4 and 7. HTLV-1 proviral load (PVL) in HTLV-1+ iDCs was determined by quantitative real-time PCR. (**e**) Pie charts showing the relative abundance of unique integration sites (UISs) in MT-2 cells and HTLV-1+ iDCs isolated after co-culture with MT-2 cells. Each pie slice represents a single observed clone. Colors indicate the most abundant identical clones. The oligoclonality index (OCI) is a measure of clonal distribution, ranging from 0 (polyclonal with all clones contributing equally to PVL) to 1 (monoclonal with all infected cells belong to a single clone). DCs, dendritic cells; mDCs, mature dendritic cells; iDCs, immature dendritic cells.

Figure 5. Quantification of DC-mediated HTLV-1 transfer toward autologous CD4+T-cells via cell-to-cell contacts.

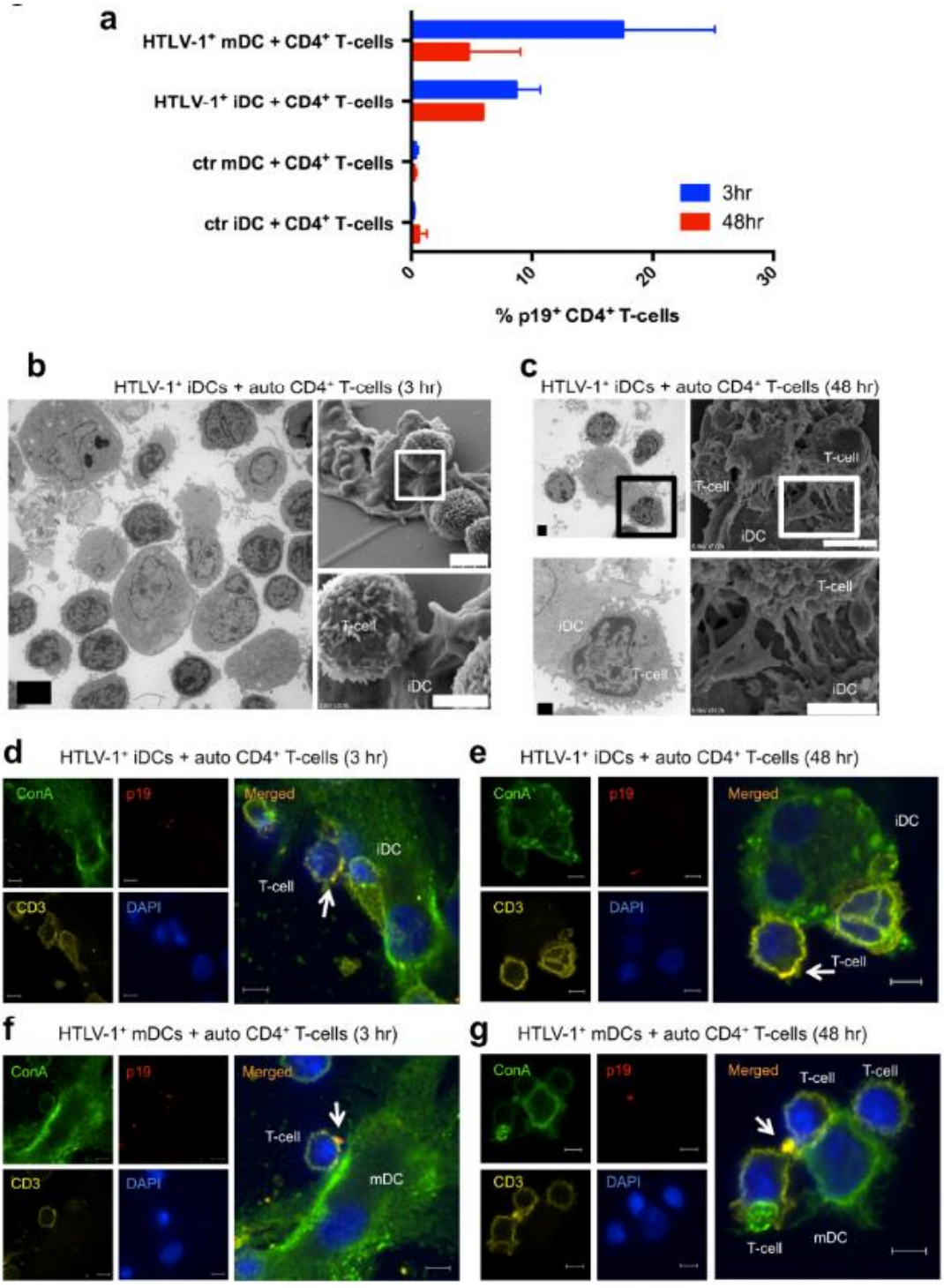

(**a**) Percentages of p19+ CD3+ CD4+ CD25– DC-SIGN– cells after co-culture with control iDCs, control mDCs, HTLV-1+ iDCs, or HTLV-1+ mDCs for 3hr or 48 hr. Data were obtained from two to three independent experiments. Error bars indicate mean ± standard deviation. (**b, c**) TEM and SEM images of cell-to-cell contacts between HTLV-1+ iDCs and autologous CD4+ T-cells after co-culture for 3 hr or 48 hr. The boxed areas in upper panels are enlarged in lower panels. Scale bars = 5 mm (left in **b**), 4 mm (right upper in **b**)**,** 2 mm (right lower in **b**), 2 mm (right upper in **c**), 1 mm (right lower in **c**), 5 mm (left upper in **c**)**,** 3 mm (left lower in **c**)**.** (**d**-**g**) Confocal immunofluorescence images of cell-to-cell contacts between HTLV-1+ iDCs/ mDCs and autologous CD4+ T-cells after co-culture for 3 hr or 48 hr. Lectin-ConA (green), p19 Gag (red), CD3 (yellow), DAPI (nucleus, blue). White arrows indicate transferred viral assemblies. Scale bars = 5 mm. iDCs, immature dendritic cells; mDCs, mature dendritic cells; TEM, transmission electron microscopy; SEM, scanning electron microscopy; ConA, Concanavalin A.